04,07

Ab initio studies of the effect of pressure on the structure, electronic and elastic properties of carbonates of alkali-alkaline earth metals

© Yu.N. Zhuravlev

Kemerovo State University,
Kemerovo, Russia

E-mail: zhur@kemsu.ru

Received May 25, 2022
Revised July 19, 2022
Accepted July 19, 2022

Density functional theory with a gradient PBE functional and dispersion correction D3(BJ) in the basis of localized orbitals of the CRYSTAL17 package was used to study the effect of pressure on the structural, electronic, and elastic properties of $K_2Ca(CO_3)_2$, $K_2Mg(CO_3)_2$, $Na_2Ca_2(CO_3)_3$, $Na_2Mg(CO_3)_2$. The parameters of the third-order Birch–Murnaghan equation of state are determined, and it is shown that the equilibrium volume and compressibility modulus depend linearly on the average cation radius. Under pressure, the widths of the upper valence bands increase maximally in $K_2Ca(CO_3)_2$ and minimally in $Na_2Ca_2(CO_3)_3$, while the centers of gravity of the cationic states shift by ~ 0.2 eV. Elastic constants and polycrystalline moduli are calculated, which increase with decreasing average cation radius. The shear modulus for $K_2Ca(CO_3)_2$ and $K_2Mg(CO_3)_2$ decreases with increasing pressure, and this leads to anomalous behavior of the longitudinal and transverse acoustic wave velocities.

Keywords: *ab initio* calculations, buchliite, eithelite, shortite, equation of state, elastic moduli, density of states, pressure.

DOI: 10.21883/PSS.2022.11.54193.386

1. Introduction

Carbonates of alkaline, alkaline-earth metals are important in partial melting of the mantle matter, metasomatic processes, diamond formation and in the deep carbon cycle [1–3]. They can be interesting from the practical viewpoint for solving the problem of carbon dioxide emission reduction by its trapping and sequestration. The result of chemical reactions with MgO, CaO oxides with the participation of Na_2CO_3, K_2CO_3 is the formation of double salts $Na_2Mg(CO_3)_2$, $K_2Mg(CO_3)_2$ [4,5]. Moreover, systems $K_2CO_3-CaCO_3$, $Na_2CO_3-CaCO_3$ are important in the material science, as a source of new materials having nonlinear optical properties [6].

Double carbonates of natrium alkaline sodium (Na), potassium (K) and alkaline-earth magnesium Mg, calcium Ca metals exist in nature in the form of minerals: butschliite (potassium-calcium carbonate with the chemical formula $K_2Ca(CO_3)_2$), eitelite (sodium-magnesium carbonate with the chemical formula $Na_2Mg(CO_3)_2$), shortite (sodium-calcium carbonate with the chemical formula $Na_2Ca_2(CO_3)_3$). $K_2Mg(CO_3)_2$ does not occur in nature and is man-made. At the atmospheric pressure, $K_2Ca(CO_3)_2$ and $K_2Mg(CO_3)_2$ crystallize into a trigonal lattice with space group $R3m$ (N 166) [7,8], $Na_2Mg(CO_3)_2$ — into a lattice with symmetry $R\bar{3}$(N 148) [9]. The butschliite and eitelite topologies are similar, but a different orientation of carbonate groups and different coordination polyhedra of alkaline metals cause the presence or absence of a mirror plane. Shortite has an orthorhombic structure with space group $Amm2$ (N 38) [10].

The studies of the phase diagrams of double carbonates at high pressures make it possible to reveal several new crystal phase states [11], which still have to be discovered [12]. That's why structural properties of double crystals under pressure were studied using synchrotron radiation in [13], where it was shown that compressibility of potassium (sodium)–magnesium carbonates is lower than that of magnesite and dolomite, while $K_2Mg(CO_3)_2$ transforms into the monoclinic polymorphous form at 8.05 GPa. The research in [14] has shown that eitelite is a stable polymorphous modification, at least up to 6.6 GPa. Shortite behavior under pressure was studied in [15], where it was found that a shortite-II phase with symmetry group Pm forms at pressures above 15 GPa, and in the range of 12–30 GPa a shortite-III phase crystallizes (its symmetry group has not been determined yet). Elastic, thermodynamic and dynamic properties of shortite, including those under pressure, were studied by theoretical methods in [16].

Electronic properties of carbonates with the calcite or dolomite structure were studied by the method of X-ray spectrum microprobe analysis in [17]. However, there were no experimental and microscopic studies of structural, electronic and elastic properties of double carbonates with the butschliite and eitelite structure under pressure. That's why in the present paper we use the ab initio methods of the density functional theory (DFT) with different functionals and bases of localized orbitals to calculate the crystal structure, band structure and densities of electronic states, elastic constants and moduli of $K_2Ca(CO_3)_2$, $K_2Mg(CO_3)_2$, $Na_2Ca_2(CO_3)_3$ and $Na_2Mg(CO_3)_2$ in the pressure range from atmospheric (0 GPa) to 10 GPa.

2. Calculation method

The structure and electronic properties of metal carbonates were studied by density functional theory methods in the CRYSTAL17 software package [18]. Crystal orbitals are assigned by linear combinations of the Bloch functions, determined in terms of localized atomic orbitals of the Gaussian type, the exponent and coefficients of which are determined from an all-electron set for atoms of carbon, oxygen, magnesium, calcium in [19], sodium, potassium [20].

Calculations were performed in a generalized gradient approximation with PBE functional [21]. We also used the PBESOL gradient functional [22], hybrid PBESOL0, with an exchange-correlation functional [22] and a 25% Hartree–Fock exchange, as well as the B3LYP hybrid functional which combines a 20% Hartree–Fock exchange with BECKE exchange functional [23] and LYP correlative functional [24], which has been successfully used earlier [25,26] in calculations of vibration properties of alkaline-earth metal carbonates. The reciprocal space is discretized using the Monkhorst –Pack grid [27] with 216 independent **k**-points in the irreducible part of the Brillouin zone. Accuracy of the self-coupling procedure was not less than 10^{-9} a.u. (1 a.u. = 27.21 eV).

A correct description of non-covalent interactions requires the inclusion of effects of large distance correlation which are not available in DFT-methods. A method for accounting of the missing energy of dispersion interaction consists in an increase of the total energy calculated for the given density approximation [28]: $E_{\text{DFT-D3}} = E_{\text{DFT}} + E_{\text{disp}}$, where E_{DFT} is the conventional self-consistent Kohn–Sham energy obtained using the functional, and E_{disp} is an empirical dispersion correction. In the present study we used the well-known Grimm scheme [29], while a dispersion correction is chosen in the D3(BJ) form [30].

The tensor of elastic constants was calculated using the algorithm [31,32] according to which they can be determined as the second derivative of energy density by a pair of deformations η in the Voigt notation:

$$C_{\alpha\beta} = \frac{1}{V}\left(\frac{\partial^2 E}{\partial\eta_\alpha \partial\eta_\beta}\right)\Big|_{\eta=0},$$

where V is the unit cell volume, $\alpha, \beta = 1, \ldots, 6$ $(1 = xx; 2 = yy; 3 = zz; 4 = yz; 5 = xz; 6 = xy)$. The second derivative here is calculated numerically, as the first derivative of the analytical gradient of total energy.

The influence of pressure on the structure and electronic properties was studied using the equation of state (EoS) in the Birch–Murnaghan parameterization [33]. The equation parameters are determined using the procedure [34] by fitting the corresponding analytical expression for the calculated curves of energy and pressure dependence on unit cell volume $E(V), P(V)$:

$$E(V) = E_0 + \frac{9V_0B_0}{16}\left((x^{-2}-1)^3B_1 + (x^{-2}-1)^2(6-4x^{-2})\right), \quad (1)$$

$$P(V) = \frac{3B_0}{2}(x^{-7}-x^{-5})\left(1+\frac{3}{4}(B_1-4)(x^{-2}-1)\right), \quad (2)$$

Here $x = (V/V_0)^{1/3}$, $B_0 = -V(\partial P/\partial V)_T$ is the isothermal bulk modulus of compression and $B_1 = (\partial B/\partial P)_T$ is its first derivative by pressure at $x = 1$. Quantities E_0, V_0, B_0, B_1 are the four parameters of the equation of state (1). Their meaning is as follows: V_0 is the volume at the energy minimum, E_0 determines the depth of $E(V)$ curve, while B_0 and B_1 determine its shape. Experimental studies are often carried out using the form of equation (2), where B_1 is taken equal to 4, and then only two parameters V_0 and B_0 remain in the equation of state. This equation will be further designated as EoS BM2, and the equation in form (2) as EoS BM3.

3. Crystal structure and electronic properties of carbonates

The basis of ab initio studies is a calculation of the crystal structure, which is used for the further study of different physical and chemical properties of solid bodies. An important role in the determination of the structure in the density functional theory is played by the selection of functionals. The accuracy of their application was estimated using root-mean-square deviations Δ of the obtained theoretical values from the experimental values of unit cell constants and nonequivalent interatomic distances K(Na)-O, Ca(Mg)-O and C-O. In $K_2Ca(CO_3)_2$ the root-mean-square deviation for six structural parameters for the functional PBE-D3 is equal to 0.63%, PBESOL — 1.18%, PBESOL0 — 1.42%, B3LYP — 1.28%. The B3LYP functional with dispersion correction D3 yields the greatest deviation of 1.46%. The root-mean-square deviations in the same sequence of functionals for $K_2Mg(CO_3)_2$ are equal to 0.48, 0.81, 1.14, 1.52%. Thereat, the PBESOL, PBESOL0 functionals yield underestimated values of the unit cell volume: in $K_2Ca(CO_3)_2$ it is 445.79, 440.65 Å^3, respectively, while B3LYP, on the contrary, yields overestimated values — 470.09 Å^3. The B3LYP-D3 method reduces the volume to 440.861 Å^3, which, however, is considerably less than in the experiment. Along with that, hybrid functionals provide a better match of C-O distances, which is important for calculating the atomic vibration frequencies.

In the present paper we use the basis of localized orbitals and to check its influence on the obtained results also use a POB-DZVP set [35], which contains a greater number of Gaussian distributions than that in [19,20] and takes into account the polarization effects. Using this basic set, the root-mean-square deviations in the same sequence of functionals for $K_2Ca(CO_3)_2$ are equal to 1.43, 1.52, 1.42, 1.27% and for $K_2Mg(CO_3)_2$ — 1.21, 1.34, 1.42, 1.53%. Thus, this basic set does not provide the best results. Deviations Δ for the PBE-D3 and B3LYP functionals for $Na_2Mg(CO_3)_2$ with seven and $Na_2Ca_2(CO_3)_3$ with nineteen non-equivalent crystallographic parameters are equal to 0.79,

Table 1. Lattice constants a, b, c, unit cell volume V, average interatomic distances of metal M (K, Na) and oxygen O, metal M1 (Ca, Mg) and oxygen, carbon C and oxygen calculated by the PBE-D3 method and measured experimentally Exp[Ref]

Method	a, Å	b, Å	c, Å	V, Å^3	M-O, Å	M1-O, Å	C-O, Å
$K_2Ca(CO_3)_2$							
Exp [36]	5.3822	5.3822	18.156	455.481	2.8779	2.3214	1.2843
PBE-D3	5.3902	5.3902	18.0258	453.555	2.8670	2.3162	1.2973
$K_2Mg(CO_3)_2$							
Exp [13]	5.154	5.154	17.288	397.7	2.797	2.096	1.288
PBE-D3	5.1704	5.1704	17.1834	397.815	2.7913	2.0993	1.2975
$Na_2Ca_2(CO_3)_3$							
Exp [15]	4.9571	11.0514	7.1242	390.28	2.4481	2.5061	1.2914
PBE-D3	4.9585	11.0801	7.0977	389.956	2.4422	2.5032	1.2965
$Na_2Mg(CO_3)_2$							
Exp [13]	4.939	4.939	16.382	346.0	2.6287	2.077	1.282
PBE-D3	4.9575	4.9575	16.2766	346.432	2.6275	2.0810	1.2960

0.87% and 0.55, 1.12%, respectively. Thus, the PBE-D3 calculation method is the optimal one, and Table 1 gives the theoretical and experimental crystalline parameters of carbonates obtained using it.

Each potassium atom in the crystal structure of butschliite is surrounded by six oxygen atoms at the distance of 2.822 Å and three oxygen atoms at the distance of 2.957 Å. The radius of a potassium cation whose charge according to the Mulliken scheme is equal to $+0.92|e|$, e — the electron charge, is equal to 1.55 Å for coordination number $N_O = 9$ as per the data of [37]. Each calcium atom, in its turn, is surrounded by six oxygen atoms at the distance of 2.316 Å and the radius of its cation with the charge of $+1.68|e|$ is equal to 1.00 Å. An ion of $CO_3^{-1.76}$ carbonate has a pyramidal structure with the height of 0.012 Å and C-O distance of 1.297 Å. A magnesium ion with the charge of $+1.675|e|$ in $K_2Mg(CO_3)_2$ has the size of 0.72 Å [37], and the corresponding Mg-O distances decrease to 2.099 Å.

Each Na atom in the eitelite structure is surrounded by three oxygen atoms at the distance of 2.316 Å, three atoms at the distance of 2.596 Å and three more atoms at the distance of 2.971 Å, so that the ion radius for coordination number 9 is equal to 1.24 Å [37]. The octahedral environment of magnesium remains as well, while the bond length decreases to 2.081 Å. The height of the $CO_3^{-1.75}$ pyramid increases to 0.023 Å.

The structure of orthorhombic shortite significantly differs from trigonal carbonates. First of all, it has more atoms which are non-equivalent from the crystallographic viewpoint. Since the immediate environment for atom Na1 consists of two oxygen atoms O1 at the distance of 2.423 Å, four atoms O2 at the distance of 2.528 Å and two atoms O3 at the distance of 2.611 Å. The other atom Na2 has a different environment: four atoms O2 at 2.300 Å and two atoms O4 at 2.406 Å. The different coordination numbers 8 and 6 also condition the different cation charge of $+0.937$ and $+0.939|e|$ and their different ionic radii, 1.18 and 1.02 Å, respectively [37]. The calcium coordination number here increases to 9, and its environment includes one atom of oxygen O3 (2.405 Å), two atoms O4 (2.417, 2.558 Å), four atoms O2 (2.505, 2.516 Å) and two O1 (2.554 Å). The calcium ion charge is equal to $1.67|e|$ and radius is 1.18 Å [37]. Shortite has two non-equivalent carbonate groups: with lengths of C1-O1 bond 1.286 and C1-2O2 1.299 Å and a group with lengths of C2-2O4 and C2-O3 equal to 1.286 and 1.322 Å, respectively.

It has been established for carbonates of alkaline-earth metals [25] that the geometrical parameters have a linear dependence on cation radius R_M. Taking into consideration the crystallographic environment, the average cation radius in carbonates $K_2Ca(CO_3)_2$, $K_2Mg(CO_3)_2$, $Na_2Ca_2(CO_3)_2$, $Na_2Mg(CO_3)_2$ is equal to 1.367, 1.273, 1.14, 1.067 Å. Then the cell volume dependence on the radius is determined as $V(Å^3) = 22.886 + 308.69R_M$ with the correlation coefficient of 0.941.

The main crystal structure peculiarities manifest themselves in an energy distribution of electrons. Fig. 1 shows the densities of electronic states $N(E)$, i.e., the number of electrons N which have energy E. It is an integral characteristic of energy band spectrum $E(\mathbf{k})$. The energy reference point is the upper filled state, so that energies $E < 0$ correspond to occupied (valence) states, and energies $E > 0$ correspond to unoccupied (conduction) electronic states.

Nine energetically separated bands of different widths are distinguished in the valence region $N(E)$ for $K_2Ca(CO_3)_2$. The lowest band with the width of 0.09 eV and the maximum at -28.1 eV is formed by two energy bands of potassium 3s-states. The next two bands with the widths of 0.19 and 0.42 eV and the maxima at -21.7, -18.5 eV are

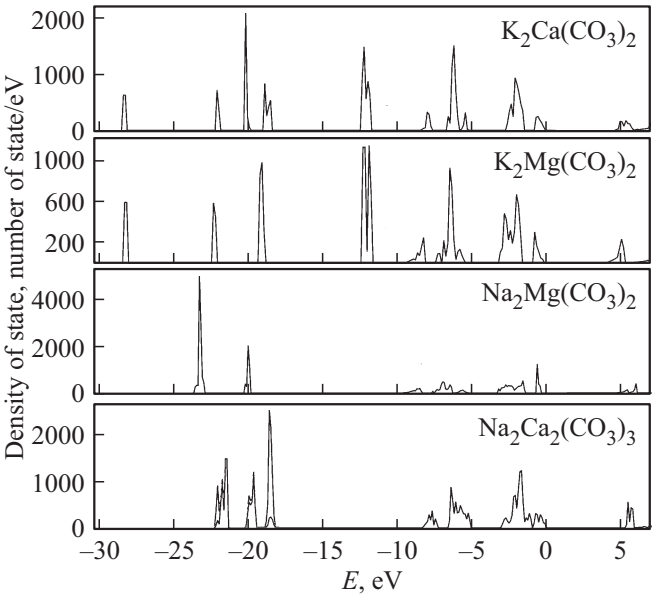

Figure 1. Density of electronic states of double carbonates.

formed by oxygen 2*s*-states with a small impurity of carbon 2*s*-states. The upper one is formed with the participation of calcium *p*-states, but their fraction does not exceed 10%. The band of calcium 3*p*-states is located in the region of -19.8 eV, its width is 0.45 eV and metal contribution is 83%. The band of 3*p*-states of now potassium with two maxima in $N(E)$ and a center of gravity on -11.9 eV has the width of 0.4 eV. This band is a reference for double carbonates with the participation of potassium.

The valence band and the lower part of the conduction band are composed of molecular states of carbonate-ions. Two and six electron energy bands are located with an energy of about -7.9 and -5.8 eV, which correspond to bonding and non-bonding crystalline orbitals composed of 72% of p_z-, p_{xy}-atomic orbitals of oxygen and 26% of carbon. The upper valence region consists of a $N(E)$ band with the width of 1.1 eV, formed chiefly by oxygen 2*p*-states, while the contribution of carbon does not exceed 3% and a band with the width of 0.6 eV, composed solely of p_{xy}-atomic orbitals of oxygen. The band gap E_g has a direct pattern, when the maximum of the valence band and the bottom of the unoccupied energy bands are within the Brillouin zone center (point Γ) and its width is equal to 4.60 eV. The states of the lower unoccupied band are formed by 4*s*-states of potassium (3%), calcium (6%), $3p_z$-carbon (54%) and oxygen (37%).

Magnesium 2*p*-states in $K_2Mg(CO_3)_2$ are located at the depth of -40.7 eV, that's why they are not shown in Fig. 1. The lower region of $N(E)$ has two bands at -22.0 and -18.9 eV with the widths of 0.2 and 0.3 eV, formed by oxygen *s*-states (68%) and carbon states (81%) respectively. The centers of gravity of potassium energy bands fall on -27.9 and -11.8 eV. The upper valence region also consists of two bands with the widths of 1.48 and 0.77 eV and energy gap of 0.73 eV between them. The band gap E_g also has a direct pattern and its width is equal to 4.08 eV.

The sodium-magnesium carbonate is characterized by an intensive and rather wide peak of 0.65 eV in the region of -21.5 eV in the valence region; this peak is formed by sodium 2*p*-states and 2*s*-hybrid states of oxygen and carbon. The region of bonding 2*s*-states of the anion falls on -18.4 eV and its width is 0.3 eV. The region of anti-bonding and bonding 2*p*-states of oxygen and carbon is located within -8.7 to -4.5 eV. The upper valence region also consists of two $N(E)$ bands: the wide one of 1.8 eV and narrow one of 0.2 eV separated by the band gap of 0.7 eV. The direct band gap at point Γ is equal to 4.60 eV, and that of the indirect one from point L(0, 0, 1/2) to point Γ has a lower energy of 4.49 eV. This differs sodium carbonates from potassium carbonates.

The peculiarities of other double carbonates manifest themselves in the valence region of $Na_2Ca_2(CO_3)_3$. The bands here are wider due to greater hybridization of cationic and anionic states, as well as the presence of non-equivalent atoms and molecular groups. Thus, the lowest energy band in Fig. 1 with the $N(E)$ peak at -21.8 eV is formed by hybrid *p*-states of atoms Na1 (16%), Na2 (6%) and *s*-states of $C1O_3$ (47%), $C2O_3$ (27%). The peak at -21.6 eV is composed by *p*- Na1 (82%) and at -21.3 eV of *p*- Na2 (88%). Thus, the difference between the two energy states of non-equivalent sodium atoms is 0.3 eV. The next band with the width of 0.67 eV and the center of gravity at -19.7 eV is by 85% composed of 3*p*-states of calcium atoms, and at -18.4 eV by hybrid states of calcium atoms (12%), atoms of $C1O_3$ (60%) and $C2O_3$ (28%).

The $N(E)$ bands in the valence band middle are traditionally formed by anti-bonding (-7.7 eV) and bonding (-5.8 eV) hybridized states of oxygen and carbon, and the states of $C1O_3$ prevail in the upper band. The upper part of the valence region with the width of 3.0 eV is formed by oxygen states and, as distinct from three other carbonates, an energy gap is virtually absent here (0.03 eV). The uppermost valence bands are formed by oxygen 2*p*-states from molecule $C1O_3$ (67%), while the lowermost unoccupied band is formed by 4*s*-states of calcium (8%) and *p*-states of carbonate group $C2O_3$ (57%). Thus, the minimum interband electronic transition is possible between two non-equivalent carbonate groups. The band gap in this compound is equal to 5.32 eV. The valence band top is at point Γ, while the bottom of the lower unoccupied band is at point *T* with the coordinates (1/2, 1/2, 1/2) in the units of reciprocal-lattice vectors.

4. Influence of pressure on structure and electronic properties

Pressure plays a significant role in the study of materials' properties [38]. Its most obvious effect is a volume decrease and, consequently, a decrease of interatomic distances in

the solid body. This, in its turn, considerably changes the electronic hybridization and chemical bond.

The influence of pressure on structural properties of carbonates is studied using the Birch–Murnaghan equations of state in form (1) — Table 2 and (2) — Table 3.

There is good agreement between the parameters of EoS BM2 calculated in the present paper and the experimental ones [13]. In [13] the obtained values of V_0, B_0 for $K_2Mg(CO_3)_2$ were 396.2 Å^3, 57.0 GPa respectively, for $Na_2Mg(CO_3)_2$ — 347.1 Å^3, 68.6 GPa. The following values were obtained in our case from equation (2) at $B_1 = 4$: 397.80 Å^3, 58.52 GPa and 346.26 Å^3, 77.45 GPa. For $Na_2Ca_2(CO_3)_3$, modulus $B_0 = 59.6$ GPa was determined for EoS BM2 in [15], from (2) it will be equal to 66.0 GPa.

The behavior of lattice constants and interatomic distances is of interest for the crystal structure study. Table 3 gives the EoS BM3 parameters for describing the dependence of pressure P on cell volume $P(V)$, lattice constants $P(a)$, $P(c)$ and for $Na_2Ca_2(CO_3)_3$ on lattice constant $P(b)$ (the second line). Fig. 2 illustrates the dependences of lattice constants a, c, cell volume V for $Na_2Mg(CO_3)_2$ on pressure P, calculated using the equation of state in form (1), (2) and measured experimentally (Exp) in [13].

An evident regularity is observed for compressibility moduli B_0: they are the greater (compressibility $k = 1/B$ is smaller), the smaller the average cation radius. For moduli B_0, from Table 2 we have $B_0(\text{GPa}) = 154.93 - 77.94R_M(0.998)$, where the correlation coefficient is given in brackets. Compressibility along the c axis for butschliite is almost 5 times greater than along the a axis, and this is explained by the fact that alternating anionic and cationic layers are located along it, while only anionic or cationic layers are located in the direction of the a axis. Rates of increase of compressibility moduli along the a axis are also from 4 to 10 times greater than for the c axis. The maximum compressibility in sodium-calcium carbonate will be observed along the c axis, and it is twice smaller for a longer b axis and a shorter a axis.

Similar values of the EoS BM3 parameters as in Table 3 were also obtained for interatomic distances. The corresponding equilibrium average distances for metal–oxygen M-O (M: Na, K) and M1-O (M1: Mg, Ca) and C-O should be taken from Table 1, while an ordinary dependence exists for compressibility moduli: $B_{0,\text{M-O(GPa)}} = 423.5 - 219.1R_M(0.989)$, $B_{0,\text{C-O(GPa)}} = 2132.1 - 837.1R_M(0.967)$. This regularity is not observed for compressibility moduli of M1-O distances, and they change as 177.0, 210.5, 191.7, 246.2 GPa with a decrease of the average cation radius. Their numerical values are greater than those for M-O distances and, consequently, compressibility is lower. This is related to a higher energy of electrostatic interaction between calcium and oxygen ions than that of potassium ions (which have a smaller charge) and oxygen. As pressure rises, the potassium charge does not change, calcium and oxygen charges slightly decrease in absolute magnitude. The linear compressibility modulus of 194 GPa for a short K-O(6) bond in $K_2Ca(CO_3)_2$ is almost three times larger than for a long K-O(3) bond (78 GPa). In $K_2Mg(CO_3)_2$ they correlate as 233 GPa to 79 GPa. On the contrary, in sodium-magnesium carbonate the longest Na-O(3) bond is virtually incompressible ($B_0 = 802$ GPa), while the average one decreases with pressure very rapidly ($B_0 = 97$ GPa, $B_1 = 19.2$). The pyramid height in butschliite decreases insignificantly, while in eitelite in increases at $P = 5$ GPa to 0.024 Å.

When pressure increases, there is a common tendency to electron delocalization, which leads to an electron band enhancement and band gap decrease. The structure of band energy spectra and spectra of density of states $N(E)$ for double carbonates under pressure does not change qualitatively. Its lower part in the upper valence region of $K_2Ca(CO_3)_2$ increases at 5 GPa to 1.34 eV (+20.7%), and the upper part increases to 0.76 eV (+17%). When pressure increases to 2 GPa, the band gap slowly in-

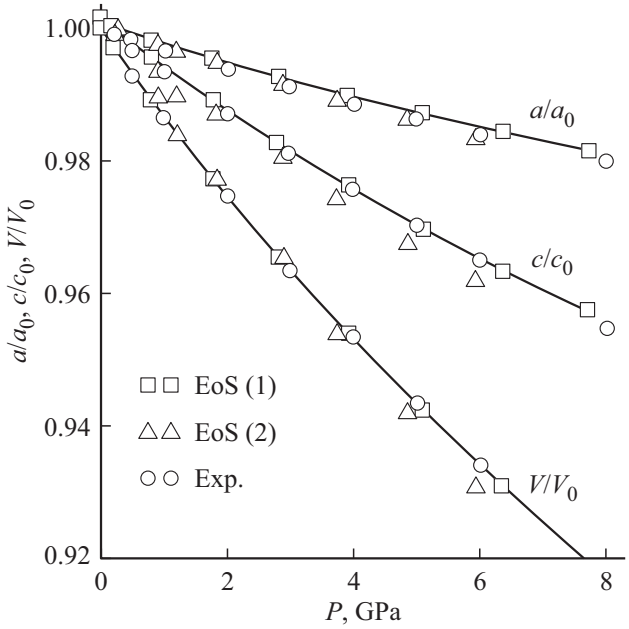

Figure 2. Dependences of ratios of lattice constants a, c, cell volume V to their equilibrium values a_0, c_0, V_0 on pressure P, calculates from the equation of state (EoS) in forms (1) (squares), (2) (triangles) and measured experimentally (Exp) (circles) in [13] for $Na_2Mg(CO_3)_2$.

Table 2. Parameters of the Birch–Murnaghan equation of state in form (1): E_0 — total energy, V_0 — equilibrium volume, B_0 — bulk modulus of compression, B_1 — its pressure derivative

Carbonate	E_0, a. u.	V_0, Å^3	B_0, GPa	B_1
$K_2Ca(CO_3)_2$	−2404.5167	453.454	48.94	5.11
$K_2Mg(CO_3)_2$	−1927.0898	397.885	55.15	5.43
$Na_2Ca_2(CO_3)_3$	−2470.7560	389.813	65.38	4.26
$Na_2Mg(CO_3)_2$	−1052.0781	346.559	72.47	5.71

Table 3. Parameters of the Birch–Murnaghan equation of state in form (2) for describing the pressure dependence on cell volume $P(V)$, lattice constants $P(a)$ (b — the second line is for sodium-calcium carbonate), $P(c)$

Carbonate	V			$a(b)$			c		
	V_0, Å^3	B_0, GPa	B_1	a_0, Å	B_0, GPa	B_{1a}	c_0, Å	B_{0c}, GPa	B_{1c}
$K_2Ca(CO_3)_2$	453.512	49.45	4.56	5.389	317.99	53.56	18.029	71.67	5.16
$K_2Mg(CO_3)_2$	397.827	56.36	5.01	5.170	385.12	40.45	17.187	79.54	7.02
$Na_2Ca_2(CO_3)_3$	389.880	64.93	4.32	4.957	286.28	23.79	7.097	123.10	5.57
				11.080	254.69	39.74			
$Na_2Mg(CO_3)_2$	346.362	73.36	5.44	4.956	299.69	32.36	16.282	141.67	8.71

creases to the value of 4.61. At pressures above 2 GPa, the band gap starts decreasing according to the law $E_g(\text{eV}) = 4.60 + 0.0081P - 0.0025P^2$. The valence bands in $K_2Mg(CO_3)_2$, which has a similar structure, increase by 13.5 and 12.9% respectively, while the band gap linearly decreases at the rate of -0.0027 eV/GPa. The same behavior is noted for the energy bands in sodium-calcium carbonate, where $E_g(\text{eV}) = 5.32 - 0.0043P + 0.0002P^2$ decreases, and the lower part of the upper valence band increases from 2.11 to 2.19 eV, the upper one — from 0.90 eV to 0.95 eV. Valence band widths in $Na_2Mg(CO_3)_2$ also increase by 8 and 33%, while the band gap here, as distinct from carbonates with the butschliite or shortite structure linearly increases with the rate of 0.0095 eV/GPa.

Metal valence bands also widen due to greater hybridization with oxygen states. The corresponding widths of potassium s- and p-bands in $K_2Ca(CO_3)_2$ become equal to 0.11 and 0.5 eV at 5 GPa, while their centers of gravity shift by ~ 0.2 eV towards the valence band top. The width of the calcium p-band increases to 0.66 eV, while its share decreases to 71% and the oxygen share, on the contrary, increases to 24%. The width of the most intensive band in the region of -21.4 eV in $Na_2Mg(CO_3)_2$ increases to 0.86 eV, while the maxima of $N(E)$ in $Na_2Ca_2(CO_3)_3$ shift for each of the three sodium bands: the hybrid one by -0.1 eV, Na1 by 0.3 and Na2 by 0.2 eV.

5. Elastic properties of carbonates under pressure

Elastic properties of minerals are important in understanding of the structure and properties of the Earth and other planets [39], which is achieved by the measurements of seismic wave velocity. The measurements of elastic constants by the Brillouin spectroscopy or ultrasonic methods lead to a spread of data about minerals, which is due to the samples' different chemical composition and physical state, e.g., their porosity and contamination by impurities. Theoretical calculation methods [40] do not have these problems and can provide rather accurate predictions.

The matrix of elastic constants C_{ij} $(i, j = 1, 2, 3)$ for crystals with the butschliite structure contains six independent elastic constants, while eitelite with a lower symmetry requires one more constant, and orthorhombic shortite will have nine such constants. The elastic constants calculated in the present paper are given in Tables 4, 5. The values of their pressure derivatives C'_{ij} are also given here.

Table 4. Calculated elastic constants C_{ij} (GPa) and their pressure derivatives C'_{ij} for carbonates with the butschliite and eitelite structure

Carbonate		C_{11}	C_{33}	C_{44}	C_{12}	C_{13}	C_{14}	C_{15}
$K_2Ca(CO_3)_2$	C_{ij}	133.0	56.8	12.3	43.0	30.9	−4.6	
	C'_{ij}	9.34	4.98	−0.79	5.14	5.37	0.21	
$K_2Mg(CO_3)_2$	C_{ij}	175.3	65.3	9.8	57.2	30.5	0.89	
	$C_{'ij}$	11.32	5.66	−1.14	3.94	4.78	0.46	
$Na_2Mg(CO_3)_2$	C_{ij}	165.1	99.1	22.5	36.2	42.8	−4.2	7.8
	C'_{ij}	8.92	6.32	1.69	5.64	3.14	−0.76	−0.21

Table 5. Calculated elastic constants C_{ij} (GPa) and their pressure derivatives C'_{ij} for $Na_2Ca_2(CO_3)_3$

	C_{11}	C_{22}	C_{33}	C_{12}	C_{13}	C_{23}	C_{44}	C_{55}	C_{66}
C_{ij}	153.4	139.7	87.8	35.7	39.9	43.1	34.8	27.9	29.6
C'_{ij}	7.14	10.12	3.25	2.38	4.86	4.63	2.85	1.64	0.63

Rhombohedral carbonates have $C_{11} > C_{33}$, which agrees with the behavior of linear moduli $B_{0a} > B_{0c}$. Elastic constant C_{44} is smaller than $C_{66} = (C_{11} - C_{12})/2$, which indicates that shear deformation in the direction of the a axis is much greater than in the direction of the$c$ axis, stress being equal. Torsion constants are $C_{12} > C_{13}$, which means that tensile deformation along the c axis will be greater when stress is applied along axis $a = b$. In $Na_2Mg(CO_3)_2$ the reverse situation is observed $C_{12} < C_{13}$. In shortite, the order $C_{11} > C_{22} > C_{33}$ for longitudinal elastic constants C_{ii} $(i = 1, 2, 3)$ at 0 GPa shows that compressibility under an external stress will be greater along axes $c > b > a$, which agrees with the obtained tendency for the EoS BM3 parameters.

To ensure the mechanical stability of crystals, elastic constants shall meet certain conditions [41]. The requirements for rhombohedral crystals are: $C_{44} > 0$, $C_{11} > |C_{12}|$, $C_{33}(C_{11} + C_{12}) > 2C_{13}^2$, $C_{44}C_{66} > 2(C_{14}^2 + C_{15}^2)$. As seen

from Table 4, they are met when no pressure is applied. Elastic constants increase when pressure increases. The highest increase rate is observed for constant C_{11} and other compression–tension constants, and the lowest one — for shear constants. Constant C_{44} decreases in crystals with the butschliite structure (when pressure increases) according to the law $C_{44}(\text{GPa}) = 12.3-0.79P-0.23P^2$ in $K_2Ca(CO_3)_2$ and $C_{44}(\text{GPa}) = 9.8-1.14P-0.06P^2$ in $K_2Mg(CO_3)_2$, so that it becomes zero at the pressures of 5.84 GPa and 6.41 GPa, respectively, and then takes on inadmissible negative values. No limitations on mechanical stability under pressure were established for sodium-magnesium carbonate. Thus, crystals with the butschliite structure retain the trigonal structure only up to certain pressures, after which structural phase transitions must take place.

The known matrix of elastic constants C_{ij} can be used to calculate (via the reciprocal matrix of elastic flexibility (compressibility) S_{ij}) the linear moduli of elasticity B_i for the i-axis ($i = a, b, c$): $B_i = (S_{i1} + S_{i2} + S_{i3})^{-1}$, as well as the bulk modulus of elasticity of single crystal $B_R = \left(S_{11} + S_{22} + S_{33} + 2(S_{12} + S_{13} + S_{23})\right)^{-1}$. The linear moduli of elasticity for crystals with the butschliite and eitelite structure, obtained in this way, agree well with those calculated in Table 3. The moduli of elasticity of F_R single crystals obey the ordinary dependence by average cation radius $B_R(\text{GPa}) = 151.79-75.60R_M$. When pressure increases, moduli B_R increase with the rates of 5.36, 5.47, 4.53, 4.96. For linear moduli determined via elastic constants, a linear dependence exists only for B_c: $B_c(\text{GPa}) = 412.0-254.2R_M$. This indicates a special dedicated role of c in the layered structure.

Natural minerals are polycrystalline aggregates and consist of a set of single crystals with a random orientation. Their mechanical properties can be studied in two extreme cases: either on the assumption of a homogeneous local deformation or of a homogeneous local stress, known as the Voigt (B_V, G_V) [42] and Reuss approximations (B_R, G_R) [43]. The best results are obtained by the Hill averaging [44], according to which the bulk modulus and shear modulus can be determined as: $B_H = (B_V + B_R)/2$, $G_H = (G_V + G_R)/2$. The bulk modulus and shear modulus, determined via matrices of elastic constants and elastic flexibility using the formulas in [45], are given in Table 6. Here the Young moduli $E_H = 9B_HG_H/(3B_H + G_H)$ and Poisson's ratios $\mu = (3B_H - 2GB_H)/\left(2(3B_H + G_H)\right)$ are also written.

Table 6. Elastic modulus B_H, shear modulus G_H, Young modulus E_H and Poisson's ratio μ for double carbonates

Carbonate	B_H, GPa	G_H, GPa	E_H, GPa	μ
$K_2Ca(CO_3)_2$	53.9	23.9	62.4	0.307
$K_2Mg(CO_3)_2$	63.9	27.0	71.0	0.315
$Na_2Ca_2(CO_3)_2$	67.1	34.7	88.8	0.279
$Na_2Mg(CO_3)_2$	73.1	37.4	95.8	0.282

Under the standard conditions, the elastic modulus $B_H(\text{GPa}) = 134.3-57.6R_M$, shear modulus $G_H(\text{GPa}) = 87.8-47.1R_M$ and Young modulus $E_H(\text{GPa}) = 218.8-115.0R_M$ of polycrystalline carbonates increase with a decrease of the average cation radius. It is known that the shear modulus describes the plastic strength and the bulk modulus describes the breaking strength. That's why the B_H/G_H correlations makes it possible to analyze the material plasticity. If it exceeds 1.75, the material is plastic according to the empirical rule. This requirement is just for all carbonates, including in the considered pressure range.

When pressure increases, the elastic modulus B_H, as the average cation radius decreases, increases at the rates of 5.76, 5.81, 4.72, 5.15, while the shear modulus behaves differently. For carbonates with the butschliite structure, it decreases with a pressure rise with a quadratic dependence for $K_2Ca(CO_3)_2$ as $G_H(\text{GPa}) = 23.9 + 0.12P-0.30P^2$ and for $K_2Mg(CO_3)_2$ as $G_H(\text{GPa}) = 27.1-0.04P-0.16P^2$. This behavior indicates mechanical instability of these polycrystals in the range of 9–13 GPa. The shear modulus in sodium-magnesium and sodium-calcium carbonates increases at the rates of 1.97 and 1.43 respectively.

Poisson's ratio μ can formally take on values from -1 to 0.5, where the lower limit corresponds to a material which is highly compressible, while the upper one corresponds to a material which in unstable under shear deformations (or is mechanically incompressible). The calculated Poisson's ratio shows the absence of a great volume change related to deformation. When pressure increases, the Poisson's ratio increases in $K_2Ca(CO_3)_2$, $K_2Mg(CO_3)_2$ at the rates of 0.017 and 0.015 GPa^{-1} and achieves the limit value when G_H take on inadmissible negative values. It increases in sodium carbonates as well, but at the lower rate of 0.005 and 0.003 GPa^{-1}.

The obtained set of elastic moduli is useful for semi-empirical estimations of several physical properties of polycrystalline materials. Acoustic velocities in a solid body can be obtained from the bulk modulus and shear modulus, as well as its density ρ. The wave energy in an anisotropic material can propagate in two modes: longitudinal and shear (or transverse). As a rule, the faster one is the longitudinal mode where vibrations of particles are parallel to the direction of wave energy propagation. The shear mode is the slower one, vibrations of particles in it are perpendicular to the propagation direction. Acoustic velocities of longitudinal (v_p) and transverse (v_s) waves can be theoretically determined from [46]: $v_P = ((B_H + 4/3G_H)/\rho)^{1/2}$, $v_S = (G_H/\rho)^{1/2}$. Like elastic moduli, they obey an ordinary dependence: longitudinal and transverse velocities of an acoustic wave are higher for carbonates having a smaller cation radius: $v_P(\text{km/s}) = 10.475-3.48R_M$, $v_S(\text{km/s}) = 6.456-2.546R_M$. There are no experimental measurements of acoustic velocities for double alkaline–alkaline-earth carbonates, therefore, the data on the longitudinal and transverse velocity of waves for magnesite [47]:

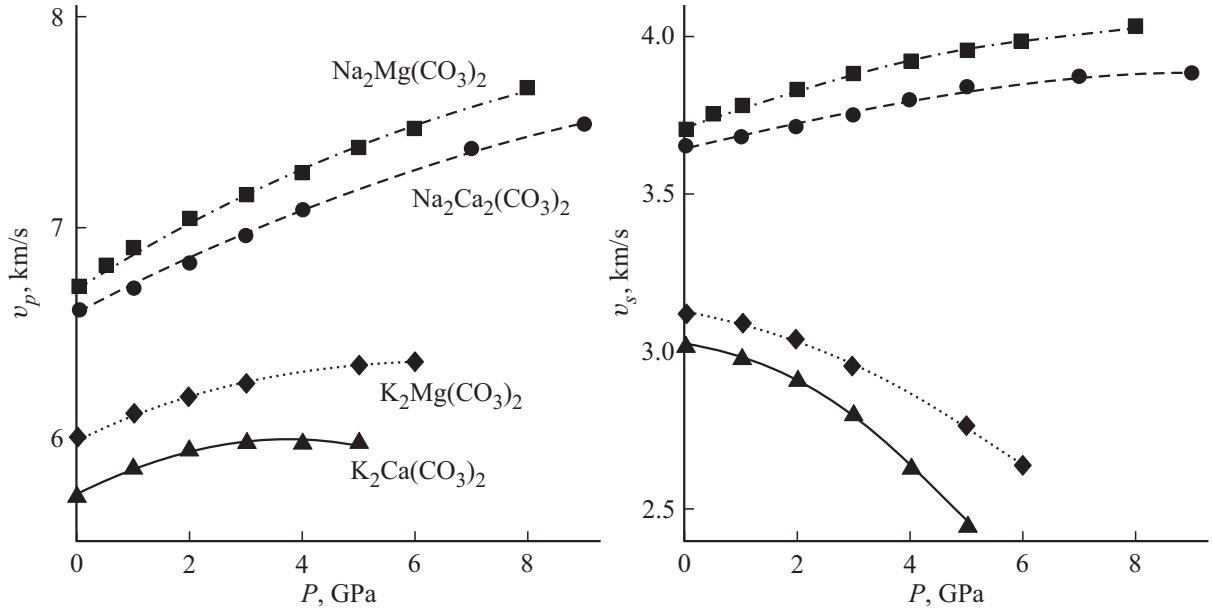

Figure 3. Dependence of longitudinal v_p (on the left) and transverse v_s (on the right) and sound velocity on pressure P for $K_2Ca(CO_3)_2$ (triangles), $K_2Mg(CO_3)_2$ (rhombi), $Na_2Mg(CO_3)_2$ (squares), $Na_2Ca_2(CO_3)_3$ (circles).

8.30, 4.81 km/s and dolomite [48] can be given for comparison: 7.05, 4.16 km/s. The velocity values obtained in the present paper for double alkaline carbonates are smaller than for alkaline-earth ones [49].

When pressure rises, the longitudinal wave velocity increases (Fig. 3), which means that the system becomes more rigid. Velocity for $K_2Ca(CO_3)_2$ first increases to 4 GPa and then decreases. The transverse component of a sound wave in eitelite and shortite increases with pressure, while in the butschliite structure in decreases, up to the anticipated phase transition point. It should be noted that such behavior of transverse waves is anomalous in the series of carbonates [50].

6. Conclusion

The methods of the density functional theory with the use of the PBE gradient functional, dispersion interaction with correction D3(BJ) in the basis of localized orbitals have been used to study the influence of pressure on structural, electronic and elastic properties of double alkaline-alkaline earth carbonates with the butschliite, eitelite and shortite structure.

The average cation radius R_M in the series of $K_2Ca(CO_3)_2$, $K_2Mg(CO_3)_2$, $Na_2Ca_2(CO_3)_2$, $Na_2Mg(CO_3)_2$ decreases as 1.367, 1.273, 1.14, 1.067 Å. For this parameter we have established an ordinary dependence of some physical characteristics of double carbonates, e.g., the parameters of the third-order Birch–Murnaghan equation of state: equilibrium volume and isothermal compressibility modulus linearly depend on cation radius $V_0(Å^3) = 23.313 + 308.33R_M$, $B_0(\text{GPa}) = 154.93 - 77.94R_M$. The following was obtained for linear compressibility moduli of M-O (M: Na, K) and C-O bond lengths: $B_{\text{M-O}}(\text{GPa}) = 423.5 - 219.1R_M$, $B_{\text{C-O}}(\text{GPa}) = 2132.1 - 837.1R_M$.

Cationic states in the energy spectrum of electrons form narrow bands in the lower part of the valence band with the following energies: $-28.1 \div -27.9$ eV, $-11.9 \div -11.8$ eV for s-, p-potassium, $-19.8 \div -19.7$ eV for p-calcium, $-21.3 \div -21.6$ eV for p-sodium. The upper valence band, formed by oxygen p-states, has an identical structure with a relatively wide lower part ($1.1 \div 2.1$ eV) and a narrow upper one ($0.2 \div 0.9$ eV) separated by a band gap of $0.03 \div 0.7$ eV. The energy distance from the upper filled state (taken as the zero energy) to the lower unoccupied state in the specified series of carbonates is equal to 4.60, 4.08, 5.32, 4.49 eV. With an increase of pressure, the band gap decreased insignificantly by $0.02 \div 0.03$ eV in crystals with the butschliite structure, remained almost unchanged in shortite and increased by 0.05 eV in eitelite.

A strong anisotropy of elastic properties has been found: linear elastic moduli along the $a(b)$ axis is approximately 5 times larger than along the c axis for crystals with the butschliite structure and two times larger in eitelite and shortite. When pressure increases, the elastic constants of compression-tension and shear increase, except C_{44}, which decreases in $K_2Ca(CO_3)_2$ and $K_2Mg(CO_3)_2$, so that it becomes zero at the pressures of 5.8 GPa and 6.4 GPa, and then it takes on the negative values which are inadmissible according to mechanical stability conditions.

The bulk modulus, shear modulus and Young modulus of polycrystalline carbonates, obtained using the Voigt–Reuss–Hill procedure, satisfy the ordinary dependence (for the cation) $B_H(\text{GPa}) = 134.3 - 57.6R_M$,

$G_H(\text{GPa}) = 87.8-47.1R_M$, $E_H(\text{GPa}) = 218.8-115.0R_M$. When pressure rises, the elastic modulus increases, while the shear modulus for carbonates with the butschliite structure decreases. Due to this, the longitudinal and transverse velocities of an acoustic wave, calculated using them, behave anomalously, and an experimental check is required.

Conflict of interest

The author declares that he has no conflict of interest.

References

[1] A.F. Shatsky, K.D. Litasov, Yu.N. Palyanov. Geologiya i geofizika **56**, *1–2*, 149 (2015) (in Russian).
[2] A. Bekhtenova, A. Shatskiy, I.V. Podborodnikov, A.V. Arefiev, K.D. Litasov. Gondwana Res. **94**, 86 (2021).
[3] I.S. Sharygin, A.V. Golovin, A.M. Dymshits, A.D. Kalugina, K.A. Solovyov, V.G. Malkovets, N.P. Pokhilenko. Dokl. RAN. Nauki o Zemle **500**, *2*, 161 (2021) (in Russian).
[4] K. Zhang, X.S. Li, Y. Duan, D.L. King, P. Singh, L. Li. International J. Greenhouse Gas Control **12**, 351 (2013).
[5] Y. Duan, K. Zhang, X.S. Li, D.L. King, B. Li, L. Zhao, Y. Xiao. Aerosol Air Quality Res. **14**, 470 (2014).
[6] Y. Song, M. Luo, D. Zhao, G. Peng, C. Lin, N. Ye. J. Mater. Chem. C **5**, *34*, 8758 (2017).
[7] A. Pabst. Am. Mineralogist **59**, 353 (1974).
[8] K.-F. Hesse, B. Simons. Z. Kristallographie **161**, 289 (1982).
[9] A. Pabst. Am. Mineralogist **58**, 211 (1973)
[10] B. Dickens, A. Hyman, W.E. Brown. J. Res. Nat. Bureau of Standards — Phys. Chem. A **75**, 129 (1971).
[11] S. Rashchenko, A. Shatskiy, K. Litasov. High-Pressure Na-Ca Carbonates in the Deep Carbon Cycle. In book Carbon in Earth's Interior. John Wiley and Sons (2020).
[12] M.R. Hazen, D.R. Hummer, G. Hystad, R.T. Downs, J.J. Golden. Am. Mineralogist **101**, 889 (2016).
[13] A. Golubkova, M. Merlini, M.W. Schmidt. Am. Mineralogist **100**, *11–12*, 2458 (2015)
[14] A. Shatskiy, P.N. Gavryushkin, I.S. Sharygin, K.D. Litasov, I.N. Kupriyanov, Y. Higo, Y.M. Borzdov, K. Funakoshi, Y.N. Palyanov, E. Ohtani. Am. Mineralogist **98**, 2172 (2013).
[15] C.E. Vennari, B.C. Meavers, Q. Williams. J. Geophys. Res.: Solid Earth. **123**, 6574 (2018).
[16] T. Inerbaev, P. Gavryushkin, K. Litasov, F. Abuova, A. Akilbekov. Vestn. Karagand. un-ta. Ser. Fizika **4**, **88**, 24 (2017) (in Russian).
[17] I.M. Kulikova, O.A. Nabelkin, V.A. Ivanov, I.A. Filenko. FTT **63**, *10*, 1505 (2021) (in Russian).
[18] R. Dovesi, A. Erba, R. Orlando, C.M. Zicovich-Wilson, B. Civalleri, L. Maschio, M. Rérat, S. Casassa, J. Baima, S. Salustro, B. Kirtman. WIREs Comput. Mol Sci. **8**, *4*, e1360 (2018).
[19] L. Valenzano, F.J. Torres, K. Doll, F. Pascale, C.M. Zicovich-Wilson, R. Dovesi. Z. Phys. Chem. **220**, *7*, 893 (2006).
[20] R. Dovesi, C. Roetti, C. Freyria Fava, M. Prencipe, V.R. Saunders. Chem. Phys. **156**, *1*, 1 (1991)
[21] J.P. Perdew, K. Burke, M. Ernzerhof. Phys. Rev. Lett. **77**, 3865 (1996).
[22] J.P. Perdew, A. Ruzsinszky, G.I. Csonka, O.A. Vydrov, G.E. Scuseria, L.A. Constantin, X. Zhou, K. Burke. Phys. Rev. Lett. **100**, 136406 (2008).
[23] A.D. Becke. J. Chem. Phys. **98**, 5648 (1993).
[24] C. Lee, W. Yang, R.G. Parr. Phys. Rev. B **37**, 785 (1988).
[25] Yu.N. Zhuravlev, V.V. Atuchin. Nanomaterials **10**, *11*, 2275 (2020).
[26] Yu.N. Zhuravlev, V.V. Atuchin. Sensors **21**, 3644 (2021).
[27] H.J. Monkhorst, J.D. Pack. Phys. Rev. B **13**, 5188 (1976).
[28] S. Grimme, A. Hansen, J.G. Brandenburg, C. Bannwarth. Chem. Rev. **116**, *9*, 5105 (2016).
[29] S. Grimme, J. Antony, S. Ehrlich, H. Krieg. J. Chem. Phys. **132**, 154104 (2010).
[30] S. Grimme, S. Ehrlich, L. Goerigk. Comp. Chem. **32**, *7*, 1456 (2011).
[31] W.F. Perger, J. Criswell, B. Civalleri, R. Dovesi. Comp. Phys. Commun. **180**, 1753 (2009).
[32] A. Erba, A. Mahmoud, R. Orlando, R. Dovesi. Phys. Chem. Minerals. **41**, 151 (2014).
[33] F. Birch. J. Geophys. Res. **83**, *3*, 1257 (1978).
[34] A. Erba, A. Mahmoud, D. Belmonte, R. Dovesi. J. Chem. Phys. **140**, *12*, 124703 (2014).
[35] T. Bredow M.F. Peintinger, D.V. Oliveira. J. Comput. Chem. **34**, *6*, 451 (2013).
[36] H. Effenberger, H. Langhof. Acta Crystallographica C **40**, *7*, 1299 (1984).
[37] R.D. Shannon. Acta Crystallographica A **32**, 751 (1976).
[38] L. Zhang, Y. Wang, J. Lv, Y. Ma. Nature Rev. Materials **2**, 17005 (2017).
[39] J.A. Ross, M. Alvaro, F. Nestola. Phys. Chem. Minerals **45**, 95 (2018).
[40] Z.Q. Wu, W.Z. Wang. Sci. China Earth Sci. **59**, 1107 (2016).
[41] F. Mouhat, F.-X. Coudert. Phys. Rev. B **90**, 224104 (2014).
[42] W. Voigt. Lehrbuch der Kristallphysik. Teubner, Leipzig. (1928). P. 978.
[43] A. Reuss. Z. Angew. Math. Mech. **9**, *1*, 4958 (1929).
[44] R. Hill. J. Mech. Phys. Solids **11**, *5*, 357 (196).
[45] Z.J. Wu, Zhao, E.J. Xiang, H.P. Hao, X.F. Liu, X.J. Meng. Phys. Rev. B **76**, 054115 (2007).
[46] O.L. Anderson. J. Phys. Chem. Solids **24**, 909 (1963).
[47] C. Sanchez-Valle, S. Ghosh, A. Rosa. Geophys. Res. Lett. **38**, L24315 (2011).
[48] J.P. Castagna, M.L. Batzle, R.L. Eastwood. Geophys. **50**, *4*, 571 (1985).
[49] Yu.N. Zhuravlev, D.V. Korabel'nikov. Mater. Today Commun. **28**, 102509 (2021).
[50] Yu.N. Zhuravlev, D.V. Korabel'nikov. Solid. State Commun. **346**, *15*, 114706 (2022).